Available online at www.ejournals.uofk.edu
UofKEJ Vol. 9 Issue 1 pp. 19- 27 (February 2020)

UNIVERSITY OF KHARTOUM ENGINEERING JOURNAL (UofKEJ)

Physical Layer Famous Waveform Approaches for Fifth Generation Cellular Network

Alzahra Hassanet, Mohamed Ali Abbas

Department of Electrical and Electronic Engineering
University of Science and Technology Faculty of Engineering, University of Khartoum
(E-mail: m_abbas111@yahoo.com)

Abstract: Many developments are taking place in the network to meet the 5G (Fifth generation) cellular network requirements; one of the very important research areas is the physical layer architecture and techniques. Studies related to the spectrum efficiency maximization indicate that the 5G air interface technology will also need to be flexible and capable of mapping various services to the best suitable combinations of frequency and radio resources.

This paper investigates the physical layer waveform approaches as part of enhanced mobile broadband use case in 5G, and finds the Cyclic-Prefix Orthogonal Frequency Division Multiplexing (CP-OFDM) as a suitable approach by comparing performance parameters where the filtering and windowing can result in degradation of the quality of the signal which is measured via Error Vector Magnitude(EVM). It also attempts to enhance the down link performance between the base station and user equipment by using power amplifier clipping technique, while modelling the downlink channel by implementing channel coding, synchronization signal burst generation, different subcarrier spacing and frame numerologies for different propagation channel and different waveform approaches.

Keywords: *Fifth Generation, Physical Layer, Waveform Approaches, Cyclic-Prefix, Multiplexing, Multicarrier.*

1. INTRODUCTION

Cellular wireless communication is one of the most advanced forms of human communication ever. The intense research has led to rapid development in the cellular communication sector in many aspects to meet the user demand [1].

The evolution of cellular wireless communications can be categorized into generations; the nomenclature of the generations generally refers to a change in the fundamental nature of the service, non-backwards-compatible transmission technology, higher spectral bandwidth and new frequency bands of development [2].

Like the previous four generations of cellular technology that each has broken backwards compatibility, Fifth Generation (5G) presents a paradigm shift that includes very high carrier frequencies with massive bandwidths, extreme base station and device densities and unprecedented numbers of antennas. But unlike the previous four generations, it will also be highly integrative: tying any new 5G air interface and spectrum together with Long Term Evolution (LTE) and WiFi especially in non-standalone phase to provide universal high-rate coverage and a seamless user experience. To support this, the radio access and core network will also have to reach unprecedented levels of flexibility and intelligence, spectrum regulation will need to be rethought and improved, and energy and cost efficiencies will become even more critical considerations [3].

The main theme of the fifth generation is the internet for everything that is, everyone and everything will be connected to the Internet. There are many emerging technologies to serve the huge number of users and to deal with the network technical aspects. The Next Generation Mobile Networks (NGMN) Alliance highlights the necessity to make more spectrums available in the existing sub-6 GHz radio bands and introduce New agile waveforms that exploit the existing underutilized fragmented spectrum, in order to satisfy specific fifth-generation (5G) operating scenarios [4]. To enable the 5G approach the assumption of synchronism and orthogonally in the network need to be investigated and introduce a broader non-orthogonal Robustness concept incorporating the overall required control signalling effort and the applied waveforms in a joint framework. For this purpose, new waveforms that carry the data on the physical layer have to be tested. The idea is to admit some crosstalk or interference, and to control these impairments by a suitable transceiver structure and transmission technique. To address these design goals various signal design techniques are used [5].

The waveform approaches are Generalized Frequency Division Multiplexing (GFDM), Universal Filtered Multicarrier (UFMC), Filter Bank Multicarrier (FBMC) and Cyclic Prefix-Orthogonal Frequency Division Multiplexing (CP-OFDM) versus the traditional Orthogonal Frequency Division Multiplexing (OFDM) or even the Filtered or windowed version of OFDM.

This paper investigates these physical layer waveform approaches as part of enhanced mobile broadband use case in 5G, by comparing performance parameters where the filtering and windowing can result in degradation of the quality of the signal which is measured via Error Vector Magnitude (EVM). It also attempts to enhance the down link performance between the base station and the user equipment by using power amplifier clipping technique, while modelling the downlink channel by implementing channel coding, synchronization signal burst generation, different subcarrier spacing and frame numerologies for different propagation channel and different waveform approaches.

August 2015, Amir Aminjavaheri and others presented a study of the candidate waveforms for 5G when they are subject to timing and carrier frequency offset. These waveforms are: orthogonal frequency division multiplexing (OFDM), generalized frequency division multiplexing (GFDM), universal filtered multicarrier (UFMC), circular filter bank multicarrier (C-FBMC), and linear filter bank multicarrier (FBMC) [6]. November 2016, Xi Zhang and others provided an overview and an in-depth analysis of the most discussed 5G waveform candidates. In addition to general requirements, the nature of each waveform is revealed including the motivation, the underlying methodology, and the associated advantages and disadvantages [7].

2017, Robin Gerzaguet and others studied a comparison of several 5G waveform candidates (OFDM, UFMC, FBMC and GFDM) under a common framework In which they assessed spectral efficiency, power spectral density, peak-to-average power ratio and robustness to asynchronous multi-user uplink transmission [8].

2.5G WAVEFORM APPROACHES

Many 5G physical layer waveform approaches are discussed in this paper, here we try to address the limitations of OFDM and find the alternatives to achieve the IMT 2020 requirements. The potential new waveforms focus on the 5G network scenarios and emerging technologies.The selected proposed approaches are discussed below:

2.1 GFDM

First we start with the generalized frequency division multiplexing (GFDM), it is a non-orthogonal, digital multicarrier transmission scheme proposed to address emerging requirements in cellular communications systems [5].

GFDM waveform is based on the time-frequency filtering of a data block, which leads to a flexible, non-orthogonal waveform. A data block is composed of K carriers and M time slots, and transmits N=K M complex modulated data [4].

It is a flexibile modulation scheme spreading the data across a two-dimensional (time and frequency) block structure (multi-symbols per multi-carriers) in contrast to the traditional orthogonal frequency division multiplexing (OFDM), it can benefit from transmitting multiple symbols per sub-carrier. GFDM targets block based transmission which is enabled by circular pulse shaping of the individual sub-carriers.

To avoid inter-symbol interference, a Cyclic Prefix (CP) is added at the end of each block of symbols. An equivalent approach with OFDM is disadvantageous due the high spectral leakage of the sinc-pulse and strict requirements to synchronization in order to maintain subcarrier orthogonality or equivalently a relatively large amount of redundant CP for relaxing the lack of synchronism.

As a generalization of OFDM, GFDM is compliant with it when the number of symbols per subcarrier is chosen to be one. It can reach OFDM Bit Error Rate (BER) performance while facilitating pulse shaped subcarriers for suppression of out of band radiation and thus minimizing interference to the legacy system when opportunistically used in white spaces. GFDM is a multi-carrier system, which digitally implements the classical filter band approach. Cyclic prefix (CP) insertion is used to allow for low complex equalization at the receiver side [5].

Mathematical description of the GFDM transceiver is given by the following equations:

Let d [k, m] be a complex valued information symbol. The K × M matrix.

$$D = \begin{bmatrix} d[0,0] & \cdots & d[0,M-1] \\ \vdots & \ddots & \vdots \\ d[K-1,0] & \cdots & d[K-1,M-1] \end{bmatrix} \quad (1)$$

The matrix will be addressed as one information block. Therein, k = 0… K−1 shall denote a subcarrier while m = 0… M−1 refers to a time slot. With the intention to distribute the data symbols in time and frequency, the discrete impulse response of the pulse shaping transmit filter g[n] needs to be movable in those dimensions. Mathematically, the expression $g[n\text{-}mN]\ e^{j2\pi\frac{kn}{N}}$ accounts for these shifts, where given a sampling time T_S the length of one symbol in time is $T_d = NT_S$ and $1/NT_S$ denotes the spacing of two neighbouring subcarriers in frequency domain. The transmit signal

$$X[n] = \sum_{m=0}^{M-1}\sum_{k=0}^{K-1} d[k,m]g[n-mN]e^{j2\pi\frac{kn}{N}} \quad \text{where } 0 \le n \le NM \quad (2)$$

Results for one block from the superposition of all shifted impulse responses that are weighted with the respective information symbols D [k, m] see Eq.(1).

In order to be able to perform equalization at the receiver in frequency domain, x[n] is prefixed with a cyclic extension and yields $\tilde{x}[n]$, which is the signal that is sent through the radio channel. The received signal is given by

$$\tilde{Y}[n] = \tilde{x}[n]*h[n] + n[n] \quad (3)$$

Where * denotes convolution with respect to noise n[n]. Removing the CP, provides y [n] and assuming the channel response h [n], is known perfectly at the receiver, one block of K×M information symbols $\bar{Y}[n]$ is equalized by

$$\bar{Y}[n] = \text{IDFT}\left[\frac{\text{DFT}(y[n])}{\text{DFT}(h[n])}\right] \quad (4)$$

With Discrete Fourier Transform (DFT) and Inverse Discrete Fourier Transform (IDFT). However, in order to ensure the cyclic structure of y[n] that is a prerequisite to $\bar{Y}[n]$, the CP of the system requires to account for the channel, as well as the transmit and receive filter.

Assuming T_h denotes the length of the channel impulse response in time domain and Tg the length of the matched filter, and then the cyclic prefix needs to be of length $T_{CP} = 2Tg + T_h$ to prevent interference between subsequent blocks and to make Frequency Domain Equalization (FDE) possible. The resulting decrease of the data rate is of factor

$$T_b/(T_b+T_{cp}) \quad (5)$$

Fig (1) demonstrates the simulation model to investigate spectrum performance for a Generalized Frequency Division Multiplexing (GFDM) system. Performance of GFDM system is compared with that of OFDM system. the implementation is based on the Fast Fourier Transform (FFT)/Inverse Fast Fourier Transform (IFFT) algorithm in GFDM transmitter. It provides the flexibility to choose a pulse shape by changing the filter of subnet work GFDM Source. bsecause GFDM is transmitted by block, not only the pulse shaping but also the transition between blocks will influence the spectrum. See Fig (2).

2.2 UFMC (UF-OFDM)

UFMC also known as Universal Filtered –Orthogonal

Frequency Division Multiplexing (UF-OFDM) is the second waveform discussed here; it is a derivative of OFDM waveform combined with post-filtering, where a group of carriers is filtered by using a frequency domain efficient implementation. this subband filtering operation is motivated by the fact that the smallest unit used by the scheduling algorithm in frequency domain in 3rd Generation Partnership Project (3GPP) Long-Term Evolution (LTE) is a Resource Block (RB), which is a group of 12 carriers. The filtering operation leads to a lower out-of-band leakage than for OFDM [4].

The i-th UFMC sub-module, with i ϵ {1,2, ..., B}, generates the ($N+N_{filter-1}$) dimensional time-domain baseband vector xi following the UFMC design criteria for the respective sub-band carrying the complex Quadrature amplitude modulation (QAM) symbol vector (si) with dimension ni x1.

N is the required number of samples per symbol to represent all sub-bands without introducing aliasing (i.e. N depends on the overall covered bandwidth), the sample rates of the single sub-bands naturally to be aligned to each other, Nfilter the length of the filter [4]. Fig (3) demonstrates the simulation model used for uncoded BER vs Signal to Noise Ratio (SNR) measurements for a universal-filtered orthogonal frequency-division multiplexing (UF-OFDM) system, when there is another UF-OFDM system treated as interference under conditions of timing and frequency offsets.

Performance of UF-OFDM system is compared with that of OFDM system. The OFDM system is provided by setting Filter Length and Filter Coefficient to be 1. In UF-OFDM system, active subcarriers are composed of some subbands which are consisted of pilots and data. Number of subcarriers in every sub band is the same.

2.3 FBMC

The third waveform approach discussed is FBMC, which is a multicarrier system and can be described by a synthesis-analysis filter bank, i.e. a trans-multiplexer structure. FBMC waveform consists in a set of parallel data that are transmitted through a bank of modulated filters, as shown in Fig (4) where$p_{Tx}(t)$ and $p_{Rx}(t)$are respectively transmit and receive prototype filters. For subcarrier k, the filter is the prototype filter phase shifted by $e^{j2\pi f_k t}$. This phase shift in the time Domain implies a frequency shift of f_k in the frequency domain. In Fig (4), the data signal is defined by Eq. (6):

$$S_k(t)=\sum_{n=-\infty}^{\infty} S_k[n]\delta(t-nT) \qquad (6)$$

With $S_k[n]$ the data symbols for subcarrier k, T the symbol period, n the symbol number and N_c the number of subchannels.

Fig (5) demonstrates the simulation model used for BER vs SNR measurements and spectrum performance for a FBMC system in AWGN (Additive White Gaussian Noise) channel and fading channel. Performance of FBMC system is compared with that of theOFDM system with ideal synchronization and ideal channel estimation.

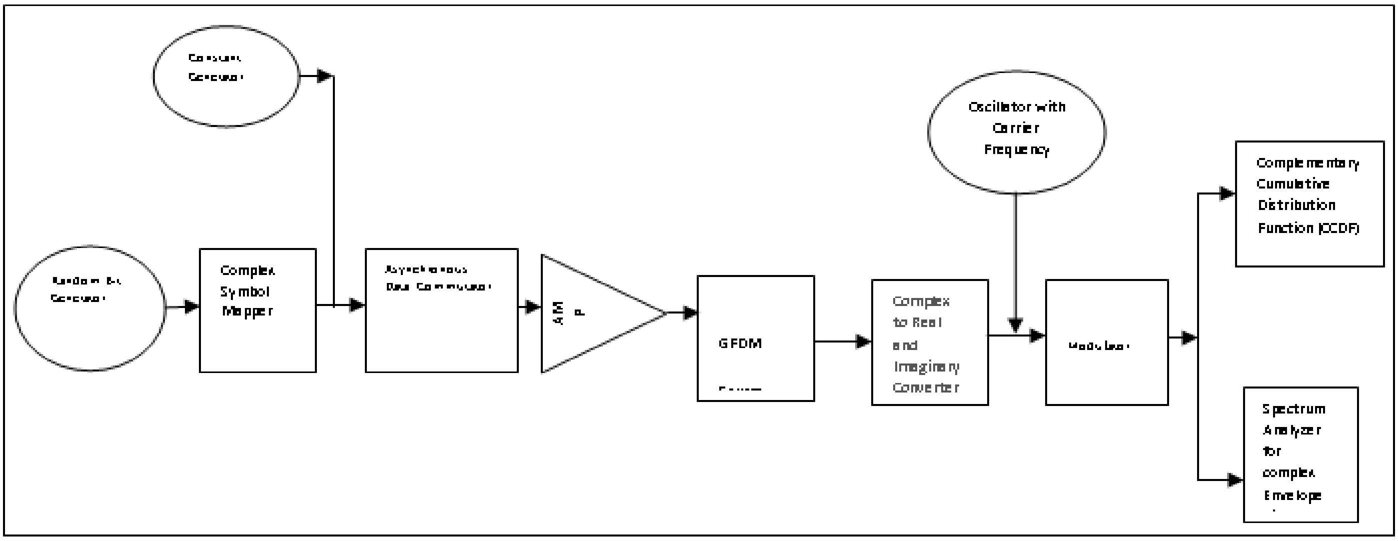

Fig. 1. GFDM Transmitter model

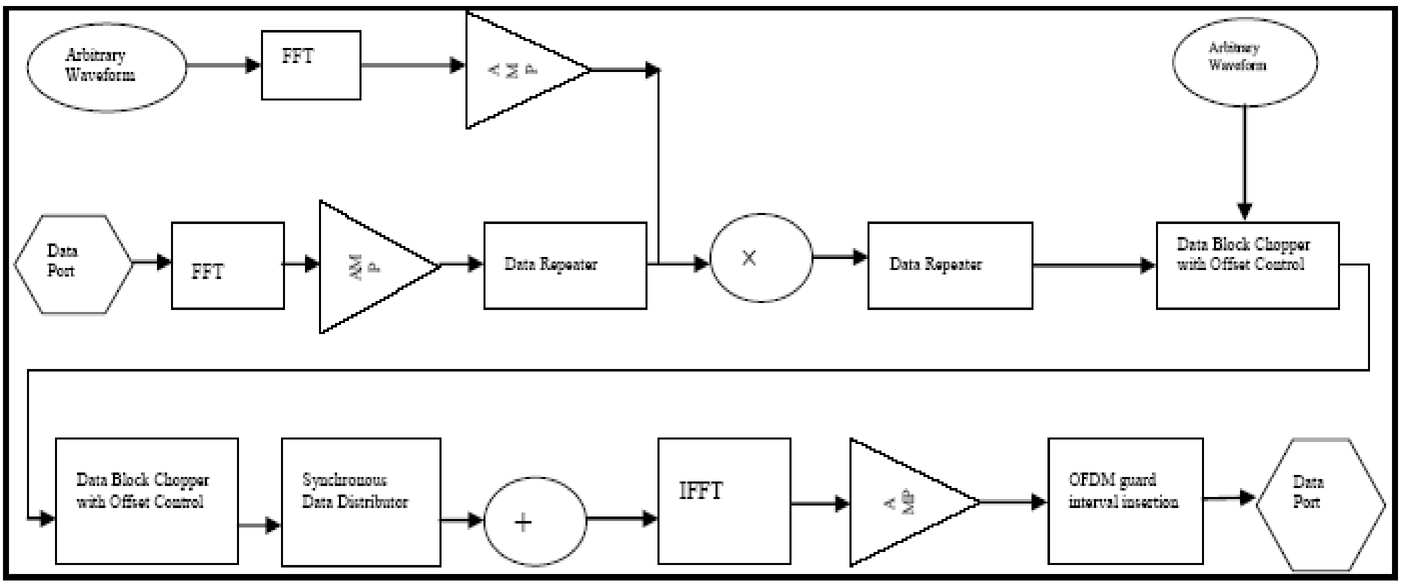

Fig. 2. GFDM Transmitter with IFFT implementation

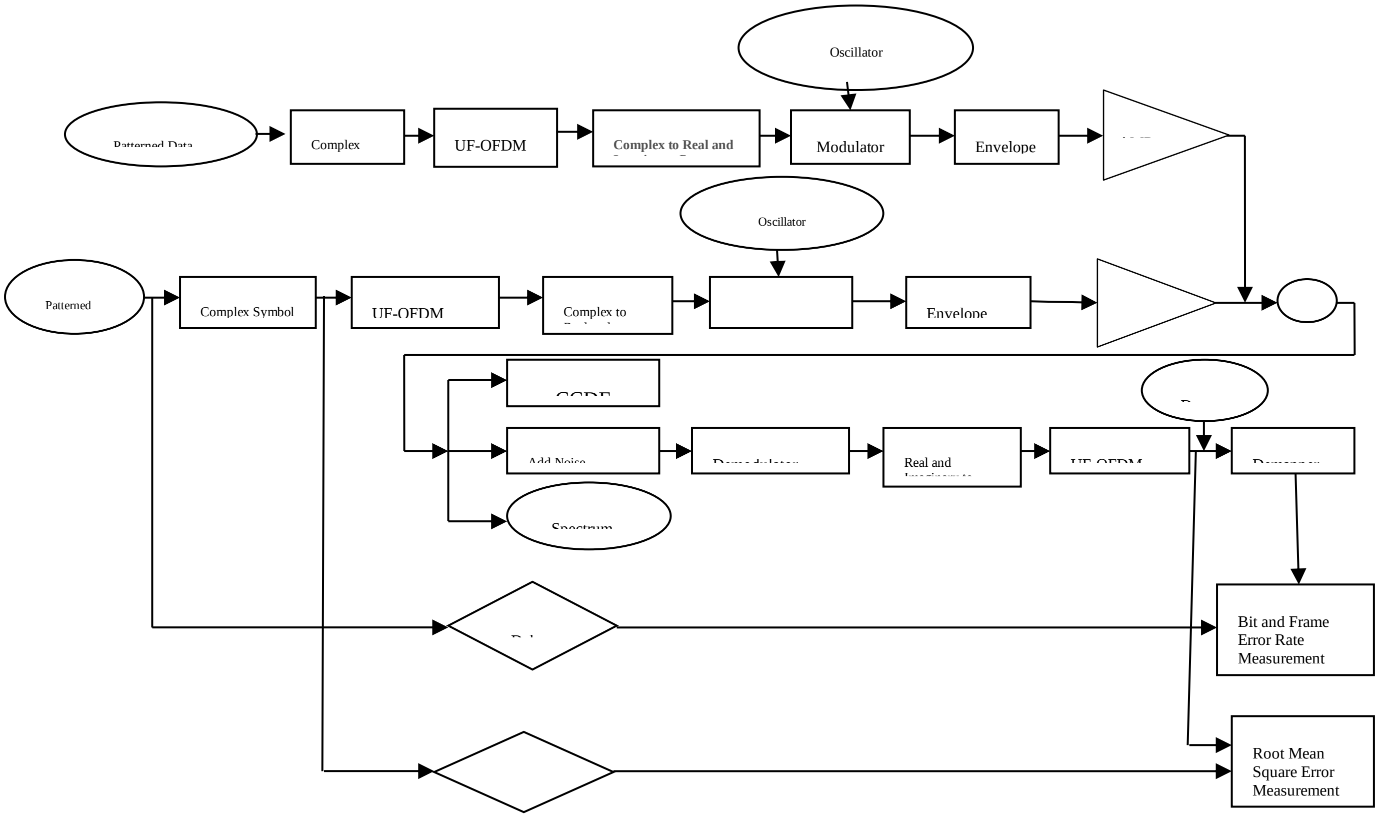

Fig. 3. UF-OFDM Simulation Model for BER Measurement

2.4 CP-OFDM

In CP-OFDM, a block of complex symbols is mapped onto a set of orthogonal carriers see Fig (6). Due to the use of inverse fast Fourier transform (IFFT) (resp. FFT) process of size N FFT, CP-OFDM architecture has a low complexity.

The principle of OFDM is to divide the total bandwidth into N FFT carriers, so that channel equalization can often be reduced as a one tap coefficient per carrier. Finally, a cyclic prefix (CP) is inserted. It guarantees circularity of the OFDM symbols, if the delay spread of the multipath channel is lower than the CP length. It, however, leads to a loss of spectral efficiency, as the CP is used to transmit redundant data. To limit the PAPR, an additional discrete Fourier transform (DFT) (resp. IDFT) a precoding stage can be inserted before the IFFT (resp. after FFT), leading to the so-called single carrier frequency division multiple access (SC-FDMA) used in the uplink of 3GPP-LTE [5].

The physical layer is the base layer and it plays an important role in achieving the transmission requirements so the physical layer modelling, design and testing are considered as the first step to take the 5G vision to reality.

3. 5G PHYSICAL LAYER

The baseband signal representing a downlink physical channel [9], [10] is defined in terms of the following steps as seen in Fig (7):

- Scrambling of coded bits in each of the code words to be transmitted on a physical channel
- Modulation of scrambled bits to generate complex-valued modulation symbols.
- mapping of the complex-valued modulation symbols onto one or several transmission layers.
- Proceeding of the complex-valued modulation symbols on each layer for transmission on the antenna ports.
- Mapping of complex-valued modulation symbols for each antenna port to resource elements.
- Generation of complex-valued time-domain OFDM signal for each antenna port.

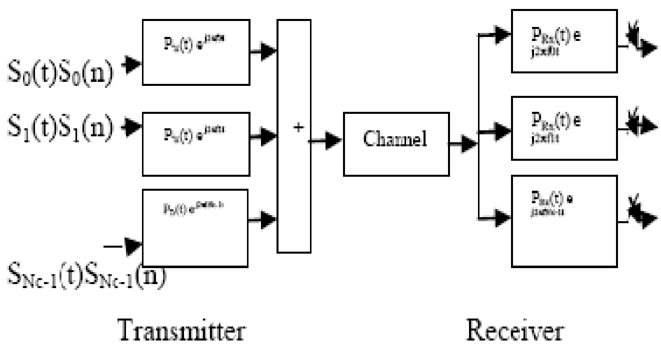

Fig. 4. Block diagram of a multicarrier transceiver [5].

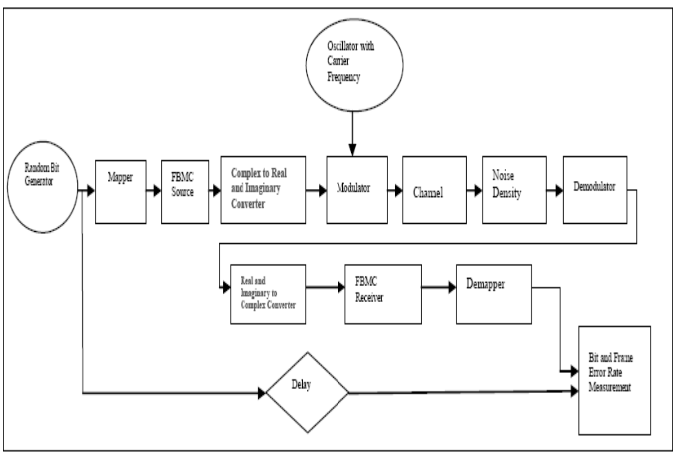

Fig. 5. FBMC Simulation Model for Measurement of Performance

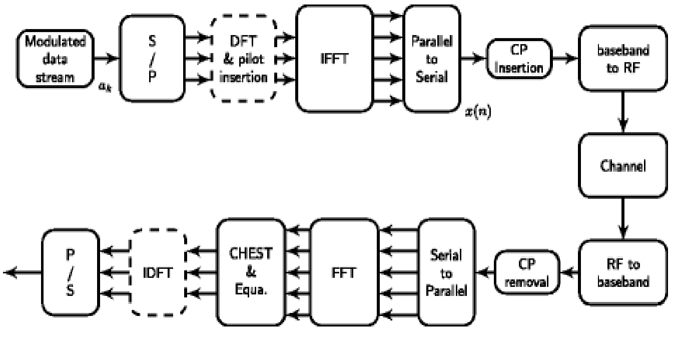

Fig. 6. CP-OFDM transceiver [4].

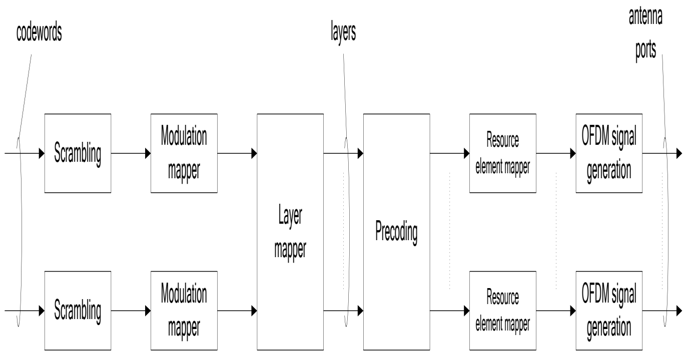

Fig. 7. Overview of physical channel processing [6].

3.1 Scrambling

For each codeword q , the block of bits $b^{(q)}(0),\ldots,b^{(q)}(M_{\text{bit}}^{(q)}-1)$, where $M_{\text{bit}}^{(q)}$ is the number of bits in codeword q transmitted on the physical channel in one subframe /slot/subslot, shall be scrambled prior to modulation, resulting in a block of scrambled bits $\tilde{b}^{(q)}(0),\ldots,\tilde{b}^{(q)}(M_{\text{bit}}^{(q)}-1)$ according to eq (7)

$$\tilde{b}^{(q)}(i) = \left(b^{(q)}(i) + c^{(q)}(i)\right) \bmod 2 \tag{7}$$

The scrambling sequence generator shall be initialized at the start of each subframe, where the initialization value of c_{init} depends on the transport channel type according to

$$c_{\text{init}} = \begin{cases} n_{\text{RNTI}} \cdot 2^{14} + q \cdot 2^{13} + \lfloor n_s/2 \rfloor \cdot 2^9 + N_{\text{ID}}^{\text{cell}} & \text{for PDSCH} \\ \lfloor n_s/2 \rfloor \cdot 2^9 + N_{\text{ID}}^{\text{MBSFN}} & \text{for PMCH} \end{cases} \tag{8}$$

Where n_{RNTI} corresponds to the Radio Network Temporary Identifier (RNTI) associated with the Physical Downlink Shared Channel (PDSCH) transmission and n_s for Physical Multicast Channel (PMCH).

For Bandwidth reduced Low complexity / Coverage Enhancement (BL/CE) User Equipment's (UEs), the same scrambling sequence is applied per sub frame to PDSCH for a given block of N_{acc} sub frames. The sub frame number of the first sub frame in each block of N_{acc} consecutive sub frames, denoted as $n_{\text{abs},1}$, satisfies $(n_{\text{abs},1}+i_\Delta) \bmod N_{\text{acc}}=0$. For the j^{th} block of N_{acc} sub frames, the scrambling sequence generator shall be initialised with

$$c_{\text{init}} = n_{\text{RNTI}} \cdot 2^{14} + q \cdot 2^{13} + \left[(j_0 + j) N_{\text{acc}} \bmod 10\right] \cdot 2^9 + N_{\text{ID}}^{\text{cell}} \tag{9}$$

Where:

$$j = 0,1,\ldots,\left\lfloor \frac{i_0 + N_{\text{abs}}^{\text{PDSCH}} + i_\Delta - 1}{N_{\text{acc}}} \right\rfloor - j_0$$
$$j_0 = \lfloor (i_0 + i_\Delta)/N_{\text{acc}} \rfloor$$
$$i_\Delta = \begin{cases} 0, & \text{for frame structure type 1 or } N_{\text{acc}} = 1 \\ N_{\text{acc}} - 2, & \text{for frame structure type 2 and } N_{\text{acc}} = 10 \end{cases} \tag{10}$$

And i_0 is the absolute sub frame number of the first downlink sub frame intended for PDSCH. The PDSCH transmission spans $N_{\text{abs}}^{\text{PDSCH}}$ consecutive sub frames including non-BL/CE DL sub frames where the PDSCH transmission is postponed.

3.2 Modulation

For each code word q , the block of scrambled bits $\tilde{b}^{(q)}(0),\ldots,\tilde{b}^{(q)}(M_{\text{bit}}^{(q)}-1)$ shall be modulated using one of the modulation schemes in Table 1, resulting in a block of complex-valued modulation symbols $d^{(q)}(0),\ldots,d^{(q)}(M_{\text{symb}}^{(q)}-1)$.

3.3 Layer mapping

The complex-valued modulation symbols for each of the codewords to be transmitted are mapped onto one or several layers. Complex-valued modulation symbols $d^{(q)}(0),\ldots,d^{(q)}(M_{\text{symb}}^{(q)}-1)$ for codeword q shall be mapped on to the layers

$$x(i) = \left[x^{(0)}(i) \quad \ldots \quad x^{(\upsilon-1)}(i)\right]^T,\ i = 0,1,\ldots,M_{\text{symb}}^{\text{layer}} - 1 \tag{11}$$

Where υ is the number of layers and $M_{\text{symb}}^{\text{layer}}$ is the number of modulation symbols per layer.

3.4 Precoding

As shown in eq (11), the precoder takes as input a block of vectors from the layer mapping and generates a block of vectors

$$y(i) = \left[\ldots \quad y^{(p)}(i) \quad \ldots\right]^T,\ i = 0,1,\ldots,M_{\text{symb}}^{\text{ap}} - 1 \tag{12}$$

To be mapped on to resources on each of the antenna ports, where $y^{(p)}(i)$ represents the signal for antenna port p .

3.5 Mapping to resource elements

For each of the antenna ports used for transmission of the physical channel, the block of complex-valued symbols $y^{(p)}(0),\ldots,y^{(p)}(M_{\text{symb}}^{\text{ap}}-1)$ shall conform to the downlink power allocation in 3GPP TS 36.213 [11] and be mapped in sequence starting with $y^{(p)}(0)$ to resource elements (k,l) which meet all of the following criteria in the current subframe:

- They are in the physical resource blocks corresponding to the virtual resource blocks assigned for transmission, and
- They are not used for transmission of the core part of PBCH, synchronization signals, and
- they are assumed by the UE not to be used for cell-specific reference signals, where the positions of the cell-specific reference signals with the number of antenna ports for and the frequency shift of cell-specific reference signals derived The mapping to resource elements (k,l) on antenna port p not reserved for other purposes shall be in increasing order of first the index k over the assigned physical resource blocks and then the index l , starting with the first slot in a sub frame.

Fig (8) shows the processing chain implemented the DM-RS and SS burst generation with the ideal synchronization and ideal channel estimation using both types of channel model CDL or TDL.

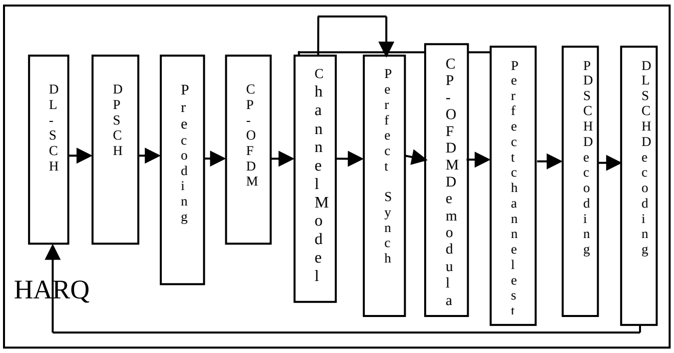

Fig. 8. Physical Layer Processing Chain

Table 1: Modulation schemes

Physical channel	Modulation schemes
PDSCH	QPSK,16QAM,64QAM, 256QAM
PMCH	QPSK,16QAM,64QAM, 256QAM

Fig (9) shows how to reserve resources for the transmission of the SS burst and how to map the signals to the resource block.

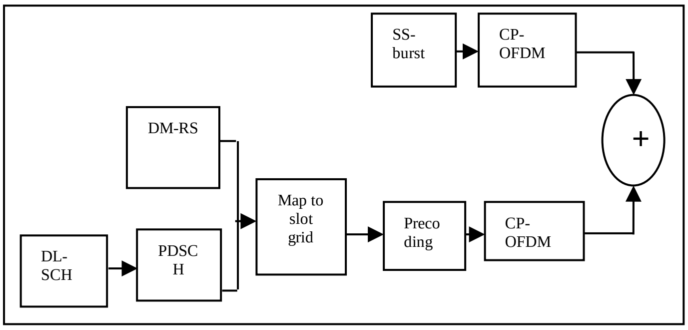

Fig. 9. Resource Block Mapping

4. SIMULATION RESULTS

4.1. GFDM

In order to achieve smooth transitions, a guard symbol (zero symbol) can be inserted into each block. As cyclic prefix (CP) would break the smooth transition, we can see the improvement introduced by guard symbol without CP.

In Fig (10) performance of GFDM system is compared with that of OFDM system.

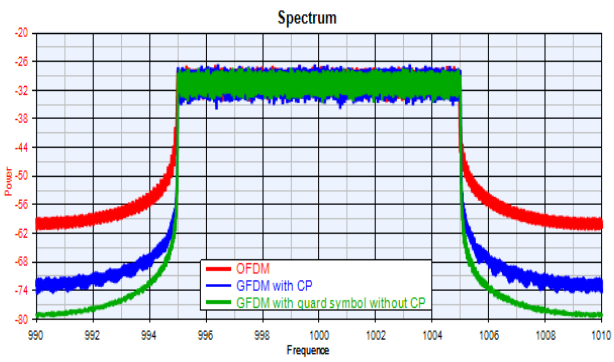

Fig. 10. OFDM Vs GFDM Spectrum (with and without CP)

4.2 UFDM

The time domain signal of every subband is passed through a filter and the transmitter signal is the superposition of all the filtered subband signals. Fig (11) provides the flexibility to choose a pulse shape by changing the filter that is controlled by filter coefficient and filter length. The filter coefficient is gotten by Chebyshev window with length 16 and Fourier transform side lobe magnitude -120 dB. The different location of every subband is implemented by multiplying the time domain data with certain frequency offset. The power of every subband is normalized. In receiver, pilots in every subband are used for channel estimation and one-dimension interpolation is done for channel response of data.

In Fig (12) of BER vs SNR one subcarrier is kept as guard between two subbands. Interference is added by multiplying the signal of interference user with frequency offset. Fig (12) simulates UF-OFDM BER performance compared to that of theory under interference conditions.

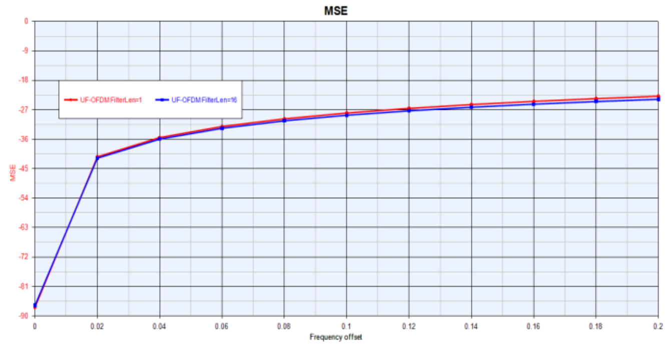

Fig. 11. UF-OFDM with Time and Frequency offset

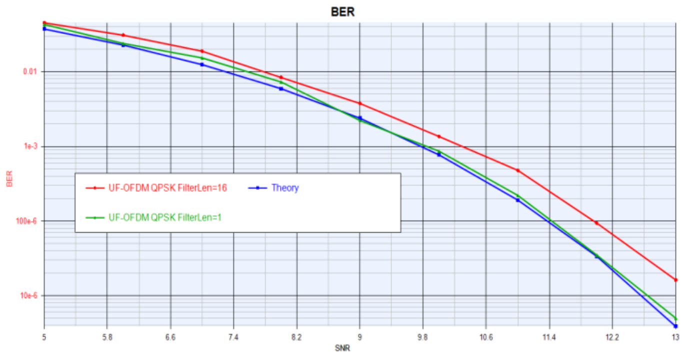

Fig. 12. Simulated UF-OFDM BER Performance

4.3 FBMC

Two implementations are given for FBMC system. The number of FFT points is extended to implement the filter bank and PPN_FFT is also provided to reduce computational complexity. OQAM is adopted in the FBMC system. The frame of FBMC is composed of preamble symbols and data symbols. Preamble consists of two superimposed ZC (Zadoff-Chu) sequences. Time & Frequency synchronization, channel estimation and equalization are done in the receiver. Fig (13) shows the BER Vs OFDM for both OFDM with ideal synchronization and FBMC using real and ideal synchronization.

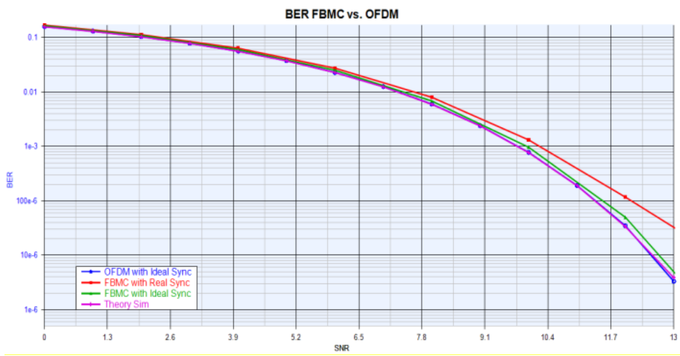

Fig. 13. BER Vs SNR for FBMC and OFDM

4.4 CP-OFDM

The simulation analyze the spectral characteristics of the following waveforms: W-OFDM,F-OFDM and CP-OFDM , these wave forms analyzed in terms of the amount of power leaked into neighbouring band and their RMS EVM, Two cases are considered : a nonlinear case where Power Amplifier (PA) non-linearity is introduced.

Fig (14) and Fig (15) show the out of band emission without PA clipping because with increased bandwidth occupancy, out of band emission have to be controlled, some windowing technique such as W-OFDM and F-OFDM is used. Fig (14) to Fig (16) show the spectrum at the band edge of a 20 MHz LTE signal(CP-OFDM) using 100 RBs and the spectrum of W-OFDM and F-OFDM signals occupying 108 RBs.

All the Figs were generated using a 513 tap filter for F-OFDM and windowing with alpha factor of 0.11. Note that the LTE signal (CP-OFDM) has been filtered to meet the LTE out of band ACLR requirements. Observe that the W-OFDM and F-OFDM waveforms use more bandwidth, potentially decreasing the spectral efficiency.

Fig (16) indicates that F-OFDM does a better job than W-OFDM in reducing the amount of out of band emissions, However when considering the non linearities of a power amplifier, the benefits of using F-OFDM against W-OFDM are reduced. Moreover the filtering operation in F-OFDM may result in higher computational complexity when compared to time domain windowing (W-OFDM).

Fig (16), Filtering and windowing can result in degradation of the quality of the signal, this is measured via EVM, the value displayed is EVM RMS.

Fig (17) shows the spectrum after using the power amplifier clipping, the selected 270 resource blocks with a subcarrier spacing of 120 kHz. This results in an occupied bandwidth of 388.8 MHz, 97.2 % bandwidth occupancy for an overall available bandwidth of 400 MHz. The main band power is approximately -70dBm and the out of band power is -140dBm.

Fig (18) shows the spectrum after using the power amplifier clipping, the selected 1080 resource blocks with subcarrier spacing of 30 kHz. This results in an occupied bandwidth of 388.8 MHz, 97.2 % bandwidth occupancy for an overall available bandwidth of 400 MHz. The main band power approximately -80dBm and the out of band power is -160dBm.

Fig (19) shows the spectrum after using the power amplifier clipping, the selected 540 resource blocks with a subcarrier spacing of 60 kHz. This results in an occupied bandwidth of 388.8 MHz, 97.2 % bandwidth occupancy for an overall available bandwidth of 400 MHz. The main band power approximately -70dBm and the out of band power is -150dBm.

Fig (20) shows the spectrum after using the power amplifier clipping, the selected 135 resource blocks with a subcarrier spacing of 240 kHz. This results in an occupied bandwidth of 388.8 MHz, 97.2 % bandwidth occupancy for an overall available bandwidth of 400 MHz. The main band power approximately -60dBm and the out of band power is -140dBm.

The second simulation measures the PDSCH throughput of a 5G link, as defined by the 3GPP NR standard. The example supports the 5G NR DL-SCH, PDSCH precoding, and 5G subcarrier spacing and bandwidths. The transmitter model includes 5G PDSCH DM-RS and SS burst. Both CDL and TDL propagation channels are supported.

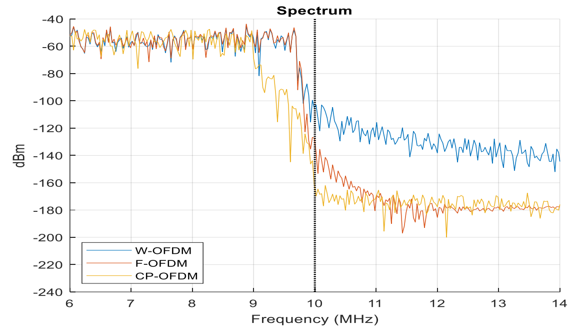

Fig. 14. Spectrum at the band edge without PA Clipping

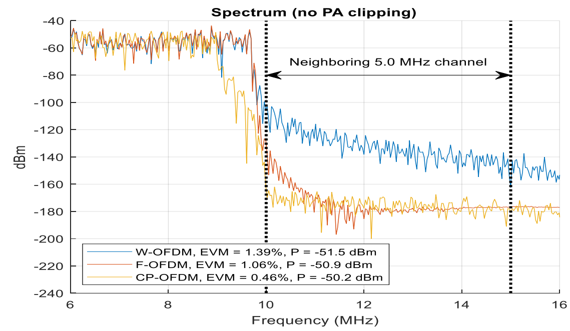

Fig. 15. Spectrum of W-OFDM and F-OFDM signals without PA Clipping

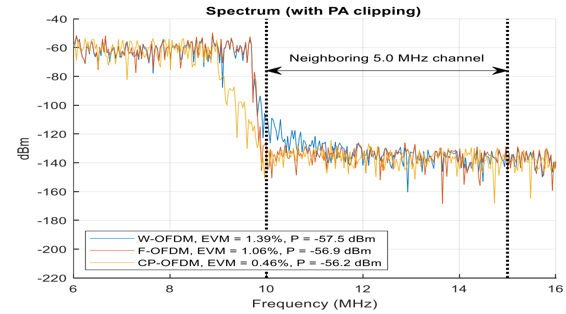

Fig. 16. Spectrum of W-OFDM and F-OFDM signals with PA Clipping

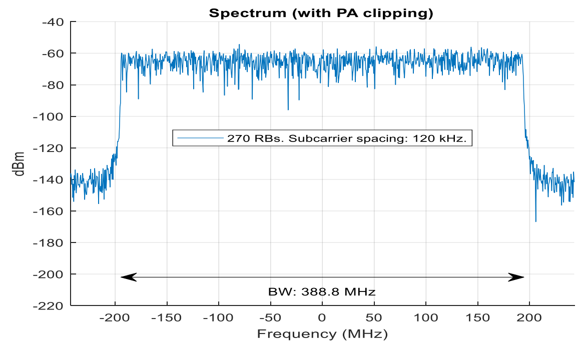

Fig. 17. Spectrum at the band edge with PA Clipping (270 RB, carrier spacing 120 KHz)

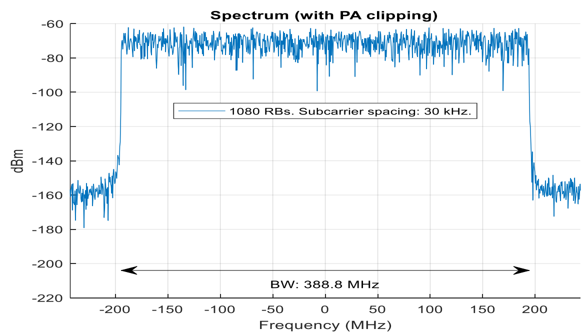

Fig. 18. Spectrum at the band edge with PA Clipping (1080 RB, carrier spacing 30 KHz)

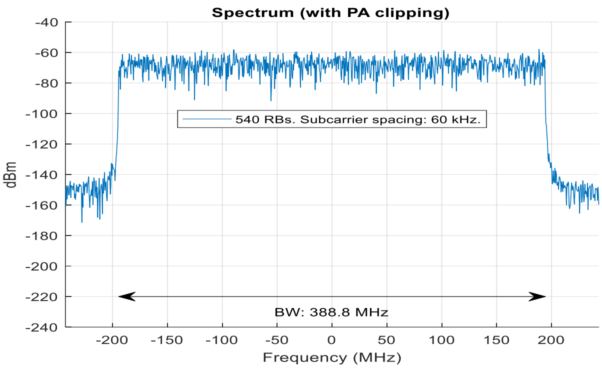

Fig. 19. Spectrum at the band edge with PA Clipping (1080 RB, carrier spacing 30 KHz)

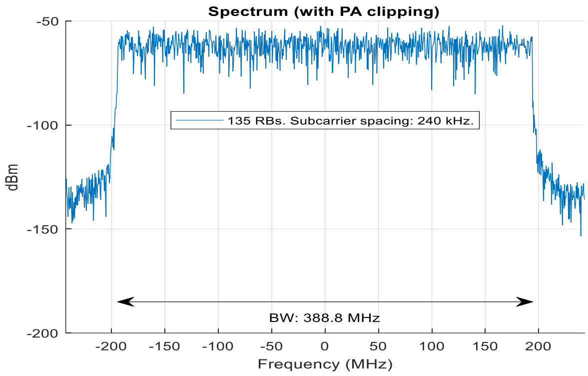

Fig. 20. Spectrum at the band edge with PA Clipping 135 RB, carrier spacing 240 KHz)

4.5 Physical layer Channel throughput

In Fig (21) and Fig (22) the perfect synchronization and perfect channel knowledge are assumed for CDL channel and CP-OFDM. The PDSCH implementation uses LTE PDSCH conFigd for non-codebook based precoding and LTE PDSCH scrambling. A single precoding matrix for the whole PDSCH allocation is determined using SVD by averaging the channel estimate across all allocated PDSCH PRBs, therefore for large PDSCH allocation, occupying a wide bandwidth, the signal processing may not be well matched to the channel across all frequencies, resulting in performance degradation. There is no beam forming on the SS/PBCH blocks in the SS burst.

In Fig (21) the subcarrier spacing is 30 kHz for 50 recourse block.

Fig 22: Subcarriers mapping to OFDM symbols, PDSCH, DM-RS, SS burst SCS=15, NDLRB=100, port=1000, (for CDL channel, CP-OFDM).

Fig (23) shows the throughput obtained when simulating 1000 frames using CP-OFDM and 8×2 MIMO and subcarrier spacing 15 kHz, CDL channel.

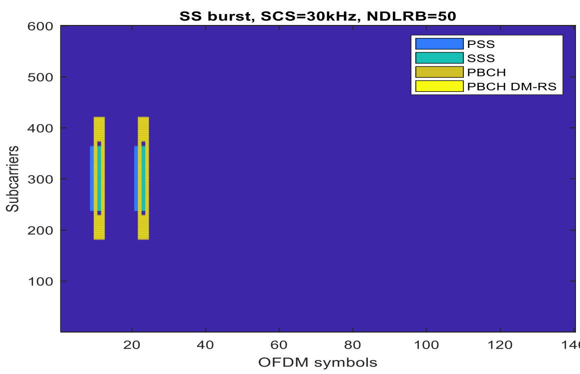

Fig. 21. Subcarriers mapping to OFDM symbols , SS burst SCS=30 , NDLRB=50(for CDL channel, CP-OFDM)

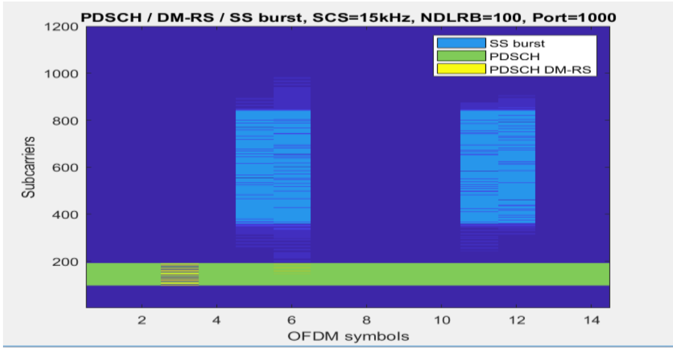

Fig. 22. the subcarrier spacing is 15 kHz for 100 recourse block.

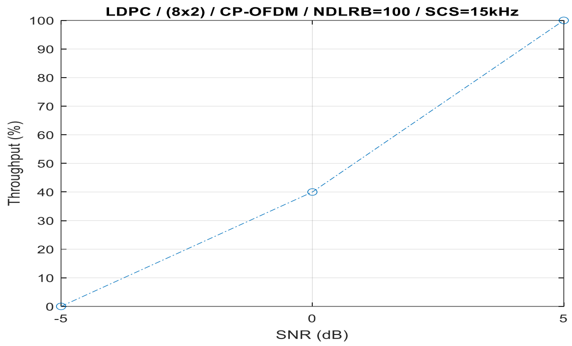

Fig. 23. Throughput vs. SNR (CDL channel, CP-OFDM)

In Fig (24) and Fig (25) perfect synchronization and perfect channel knowledge are assumed for TDL channel and CP-OFDM, there is no clear difference with respect to CDL channel.

In Fig (24) the subcarrier spacing is 30 kHz for 50 recourse block.

Fig 25: Subcarriers mapping to OFDM symbols, PDSCH, DM-RS, SS burst SCS=15, NDLRB=100, port=1000, (for TDL channel, CP-OFDM)

Fig (26) shows the throughput obtained when simulating 1000frames using CP-OFDM and 8×2 MIMO and subcarrier spacing of 15 kHz, TDL channel. The same throughput result for CDL channel.

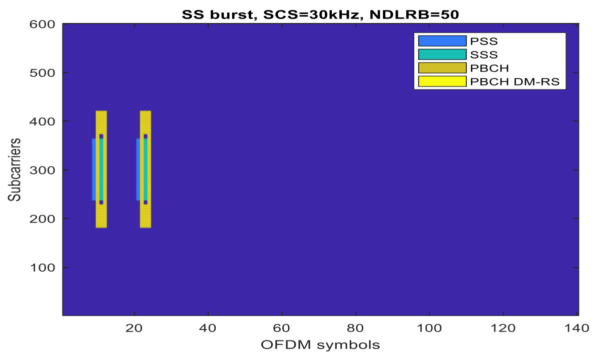

Fig. 24. Subcarriers mapping to OFDM symbols , SS burst SCS=30 , NDLRB=50(for TDL channel, CP-OFDM)

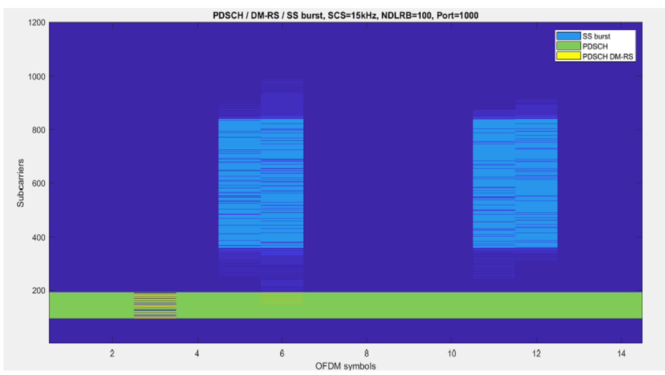

Fig. 25. the subcarrier spacing is 15kHz for 100 recourse block.

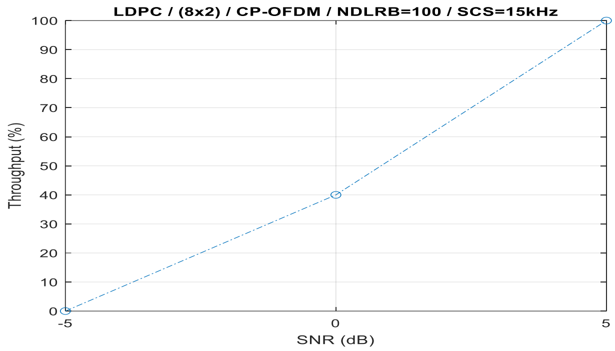

Fig. 26. Throughput vs. SNR (TDL channel, CP-OFDM)

The simulation gives the same results for the resource blocks and throughput using W-OFDM and F-OFDM.

6. CONCLUSIONS

5G will use OFDM with cyclic prefix as modulation scheme. In order to increase spectral efficiency, out of band emissions must be controlled. LTE already implements filtering and windowing to control spectral leakage. However, in LTE, a bandwidth occupancy limit of 90% is mandatory. In 5G, the 90% bandwidth occupancy limitation does not apply, potentially enabling an increase in spectral efficiency.

A comparison of several 5G multicarrier waveform candidates (OFDM, UFMC, FBMC, GFDM) has been conducted under a suitable framework. UFMC also preserves backward compatibility with well-known OFDM algorithms (channel estimation, MIMO detectors). FBMC and GFDM go a step further: interference between adjacent bands is minor, making these waveforms particularly interesting for 5G scenarios, at a price of slight complexity increase.

The F-OFDM does a better job than W-OFDM in reducing the amount of out of band emissions. However, when considering the non-linearities of a power amplifier, we can see that the benefits of using F-OFDM against W-OFDM are reduced after using the power amplifier clipping. Moreover, the filtering operation in F-OFDM may result in higher computational complexity when compared to time domain windowing (W-OFDM).

7. RECOMMENDATIONS FOR FUTURE WORK

For further researches in the 5G network especially the physical layer waveform approaches there are many points the paper recommends to be considered and they are as follows:

- Model the uplink channels and use the actual synchronization and channel knowledge and use the SS/PBCH block and PDSCH DM-RS signals at the receiver side.
- Use the 5G physical layer implementation because this paper implements the LTE PDSCH conFigd for non-codebook based proceeding and LTE PDSCH scrambling Therefore for large PDSCH allocations, that is occupying a wide bandwidth, the single preceding matrix may not be well matched to the channel across all frequencies, resulting in performance degradation. There is no beam forming on the SS/PBCH blocks in the SS burst.
- Update the HARQ process. The HARQ process either carries new transport data or a retransmission of previously sent transport data depending upon the acknowledgment (ACK) or negative acknowledgment (NACK). ACK or NACKs are not transmitted in this simulation, instead of this the CRC results signal was used. All this is handled by the HARQ scheduler, hHARQScheduling.m. The PDSCH data is updated based on the HARQ state.
- For 5G physical layer demo use Keysight Technologies, 5G New Radio Modulation Analysis, Option BHN, 89600 VSA Software.

REFERENCES

[1] Prof. S. Nandakumar, Rahul Singh and Sanjeet Singh "Traffic Driven & Received Signal Strength Adaptive Handoff Scheme", *International Journal of Computer Applications* (0975 – 8887) Volume 21– No.6, May 2011.

[2] Jiang Xie and ShantidevMohanty, "Mobility Management in Wireless Systems," in 6.108.*Telecommunication Systems and Technologies*, edited by Paolo Bellavista, in Encyclopedia of Life Support Systems (EOLSS), developed under the Auspices of the UNESCO, Eolss Publishers, Oxford, UK, 2009.

[3] Jeffrey G. Andrews, and others “What Will 5G Be?"

[4] *IEEE Journal on Selected Areas in Communications*, Special Issue on 5G Communication Systems, Editorial/Tutorial Paper, September 2014.

[5] Robin Gerzaguet,and others, “EURASIP Journal on Wireless Communications and Networking”, December 2017.

[6] 5GNOW,” 5G Waveform Candidate Selection”, ‘5GNOW_D3.1_v1.0.docx’ Version: 1.0 Last Update: 21/11/2013.

[7] Amir Aminjavaheri, and others , “Impact of timing and frequency offsets on multicarrier waveform candidates for 5G”, *IEEE Signal Processing and SignalProcessing Education Workshop (SP/SPE)*, 2015.

[8] Robin Gerzaguet, and others, “The 5G candidate waveform race: a comparison of complexity and performance”, *EURASIP Journal on Wireless Communications and Networking*, 2017.

[9] Xi Zhang, and others, “On the Waveform for 5G”, *IEEE Communications Magazine*, 2016.

[10] 3GPP Evolved Universal Terrestrial Radio Access (E-UTRA); Physical Channels and Modulation, TS 36.211. V15.2.0, 06-2018.

[11] 3GPP Evolved Universal Terrestrial Radio Access (E-UTRA); Multiplexing and channel coding, TS 36.212. V15.2.1, 07-2018.

[12] 3GPP Evolved Universal Terrestrial Radio Access (E-UTRA); Physical layer procedures, TS 36.213. V14.7.0, 06-2018.